Random lasing in strongly disordered medium

Ke Yao (姚 轲)[1], Guoying Feng (冯国英)[1*], Liling Yang (杨丽玲)[1], Jiayu Yi (易家玉)[1], Yingsong Song (宋影松)[2], and Shouhuan Zhou (周寿桓)[1,3]

[1]*Department of Opto-Electronics, Sichuan University, Chengdu 610064, China*

[2]*Institute of Applied Electronics, China Academy of Engineering Physics, Mianyang 621900, China*

[3]*North China Research Institute of Electro-Optics, Beijing 100015, China*

[*]*Corresponding author: guoing_feng@scu.edu.cn*

Received February 13, 2012; accepted March 14, 2012; posted online May 16, 2012

Using the time-dependent theory, we calculate the random-laser emission spectra in a two-dimensional strongly disordered medium. The calculation results show that in low dimensional systems, such as thin-film disordered media and planar waveguides, the larger the difference of the refractive indices between the scattering and background media, the smaller the lasing threshold. We also reveal the existence of multi-mode survival and mode competition. We experimentally obtain the emission spectra of a dye solution with Al particles doped at different pumping energies, and the experimental results agree well with the calculated ones.

OCIS codes: 290.4210, 140.3430, 300.6500.

doi: 10.3788/COL201210.082901.

In 1968, Letokhov first calculated the optical properties of a disordered medium and predicted the possibility of random lasing in disordered systems with gain. Since then, the random-laser action has been widely studied. Numerous theoretical[1−9] and experimental[10−18] investigations on random lasers have been made. Lawandy *et al.* discovered random emission in colloidal solutions in 1994[10]. Then, Cao *et al.* observed the stimulated emission phenomenon in ZnO powders[11]. With the discovery of random lasers, many theoretical explanations for such laser phenomenon have been proposed, mainly including the diffusion equation with gain[2,17]. Anderson localized model, and time-dependent theory[3,19]. Letokhov established the diffusion equations with gain and successfully explained the exponential growth of photon energy density. Jiang *et al.* proposed the time-dependent theory using the finite-difference time domain (FDTD) algorithm to solve rate and Maxwell's equations numerically[3]. Using the time-dependent theory, we intuitively and comprehensively investigated the coherent feedback properties of random emission[20,21].

In this letter, using the time-dependent theory, we calculated the dependence of random lasing on the refractive indices of the scattering media. The calculation results show that when the pumping energy is relatively small, the peak intensity of the output spectrum changes slowly with the pumping energy and the full-width at half maximum (FWHM) is relatively large. When the pumping energy is increased to a certain value, the peak intensity exhibits exponential growth and the FWHM rapidly decreases. When the pumping energy is further increased, the peak intensity and FWHM reach and maintain certain values. Thus, in low dimensional systems, the larger the difference of the refractive indices of the scattering and background media, the smaller the lasing threshold. Moreover, we observed that the number of peaks in the emission spectrum increased as the pumping energy increased. These peaks appear at different locations and pumping energies, indicating mode competition. To confirm our theoretical predictions, we performed an experiment, where we chose the Al particles as the scattering medium and the Rhodamine-6G (Rh6G) as gain medium[22]. The scattering cross section of Al particles and the module of the refractive index of the Al particles are relatively large. We mixed moderate Al particles into the Rh6G solution constituting the sample and then obtained the emission spectra at different pumping energies. The measured results agree with the calculated results.

In this letter, the system is considered a two-dimensional (2D) square disorder medium of size L^2 made of circular particles with radius r, refractive index n_2, and surface filling fraction Φ. These particles are randomly distributed in a background medium with refractive index n_1. The surface-filling fraction is defined as the ratio of the total area of particles and the area of the random system.

The background medium is chosen as the active part of the system and modeled as a four-level atomic system. Rate and Maxwell's equations are used to describe the time evolution of the atomic populations and field, respectively. To model an open system, we used perfectly matched layer absorption conditions[23]. In this simulation, the parameters are n_1=1, L=2 μm, r=60 nm, and Φ=0.3.

Two kinds of electromagnetic waves exist, namely, TM and TE. In this letter, we only consider the TM wave. In this case, Maxwell's equations can be simplified as[3]

$$\mu_0 \frac{\partial H_x}{\partial t} = -\frac{\partial E_z}{\partial y}, \tag{1}$$

$$\mu_0 \frac{\partial H_y}{\partial t} = \frac{\partial E_z}{\partial x}, \tag{2}$$

$$\varepsilon_0 \varepsilon_i \frac{\partial E_z}{\partial t} + \frac{\partial P}{\partial t} = -\frac{\partial H_x}{\partial y} + \frac{\partial H_y}{\partial x}, \tag{3}$$

where ε_0 and μ_0 are the vacuum permittivity and permeability, respectively, and $\varepsilon_i = n_i^2$ with the subscript i=1 and 2 identifying the scattering particles and gain media,

respectively.

The four-level rate equations are as[3]

$$\frac{\mathrm{d}N_1}{\mathrm{d}t} = \frac{N_2}{\tau_{21}} - W_\mathrm{p} N_1, \tag{4}$$

$$\frac{\mathrm{d}N_2}{\mathrm{d}t} = \frac{N_3}{\tau_{32}} - \frac{N_2}{\tau_{21}} - \frac{E_z}{\hbar\varpi_\mathrm{l}}\frac{\mathrm{d}P}{\mathrm{d}t}, \tag{5}$$

$$\frac{\mathrm{d}N_3}{\mathrm{d}t} = \frac{N_4}{\tau_{43}} - \frac{N_3}{\tau_{32}} + \frac{E_z}{\hbar\varpi_\mathrm{l}}\frac{\mathrm{d}P}{\mathrm{d}t}, \tag{6}$$

$$\frac{\mathrm{d}N_4}{\mathrm{d}t} = -\frac{N_4}{\tau_{43}} + W_\mathrm{p} N_1, \tag{7}$$

where P is the polarization intensity obeying the following equation:[3]

$$\frac{\mathrm{d}^2 P}{\mathrm{d}t^2} + \Delta\varpi_\mathrm{l}\frac{\mathrm{d}P}{\mathrm{d}t} + \varpi_\mathrm{l}^2 P = \kappa \Delta N E_z, \tag{8}$$

where $\Delta\varpi_\mathrm{l} = 1/\tau_{32} + 1/T_2$ is the FWHM linewidth of the atomic transition; T_2 is the mean time between dephasing events; $\Delta N = N_2 - N_3$, representing the population inversion $\kappa = (6\pi\varepsilon_0 c^3)/(\varpi_\mathrm{l}^2 \tau_{32})$; N is the total population obtained as $N = N_1 + N_2 + N_3 + N_4$. The parameters used in this work are T_2=2×10^{-14} s, τ_{43}=10^{-13} s, τ_{32}=10^{-10} s, τ_{21}=10^{-12} s, N=3.3313×10^{24}, ϖ_l=4.05×10^{15} Hz, and the corresponding wavelength λ_0=465 nm. The pumping pulse used in the numerical calculation is a Gaussian pulse, which obeys the following equation:

$$E_z(t) = \exp[-(t - t_0)^2/T^2] \cdot \cos(\omega t), \tag{9}$$

where $t_0 = 1$ fs, T=5×10^{-13} s, and ω= 4.05 × 10^{15} Hz.

In the calculations, the refractive index of the scattering particles is set to 2.5 and the radius is set to 60 nm. The calculated spectra at different pumping rates are shown in Fig. 1(a). When the pumping rate (W_p) is relatively small (∼6×10^{10} s^{-1}), the emission spectrum has a width of about 6.5 nm (centering at 464 nm) and the peak intensity is quite small. As the pumping rate increases, the emission spectrum becomes narrower and the peak intensity increases. As the pumping rate further increases, new peaks appear in the emission spectrum. As shown in Fig. 1(b), the wavelengths of new peaks depend on the pumping rate (W_p). At the pumping rate of 9×10^{10} s^{-1}, the peak wavelength λ_3 is 464 nm. When W_p is increased to 4×10^{11} s^{-1}, two distinct peaks are seen in the emission spectrum, that is, one λ_4=471 nm and the other λ_2=461 nm. When W_p reaches 9×10^{12} s^{-1}, the peaks move to λ_1=457 nm and λ_5=471 nm, respectively. As the pumping rate continues to increase, more peaks appear while some peaks also disappear. The results agree with the experimental results of Van Der Molen *et al.*[15]. Moreover, this phenomenon is due to the multiple eigenmodes in the strongly disordered random media and the different lasing thresholds of every eigenmode. In the above simulation, the mode of the wavelength at λ_3=464 nm first reaches the lasing threshold with the pumping rate increasing from a very small value. Then, it produces a peak in the emission centered at 464 nm. As the pumping rate increases, more and more modes (λ_1, λ_2, λ_4, and λ_5) reach their lasing threshold successively. However, like in a conventional laser,

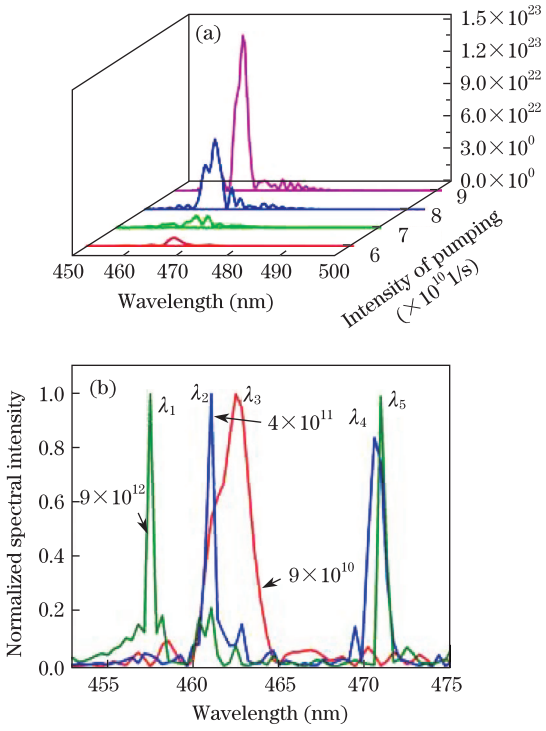

Fig. 1. (Color online) (a) Emission spectra at different pumping rates 6×10^{10} (red), 7×10^{10} (green), 8×10^{10} (blue), and 9×10^{10} s^{-1} (pink); (b) normalized emission spectra at different pumping rates 9×10^{10} (red), 4×10^{11} (blue), and 9×10^{12} s^{-1} (green). (n_2=2.5)

mode competition still exists in a random laser. Therefore, only the modes that advance in the competition can survive stably and be amplified. The other modes suppressed in the competition will be hidden or disappear in the spectra.

To clarify the influence of the refractive indices of the scattering particles on random lasing, we select three refractive indices, namely, 1.5, 2, and 2.5, respectively. Figure 2 shows the dependence of peak intensity and FWHM on pumping rate. Figure 2(a) illustrates the peak intensity and FWHM varying with the pumping rate at the refractive index of 2.5. As shown, when the pumping rate is relatively small (smaller than lasing threshold), the peak intensity is small and changes slowly with pumping rate. Moreover, the FWHM is relatively large. When the pumping rate is increased beyond a certain value (lasing threshold), the peak intensity exhibits exponential growth. Simultaneously, FWHM decreases dramatically. The peak intensity and FWHM reach a stable value when the pumping rate is further increased. When the pumping rate is small, the FWHM increases, because our pumping source is a 0.7-mm Gaussian pulse. When the pumping rate is very small, no mode oscillates. Therefore, the emission spectrum is the typical spectrum of the pumping source. Here, we use the rate equation to explain the results above. When the pumping rate is small, the population inversion is small, and hence, stimulated emission is weak. As pumping rate increases, the population inversion increases and the stimulated emission becomes stronger. The photo energy density increases. Therefore, the peak intensity increases. However, the population inversion could not increase

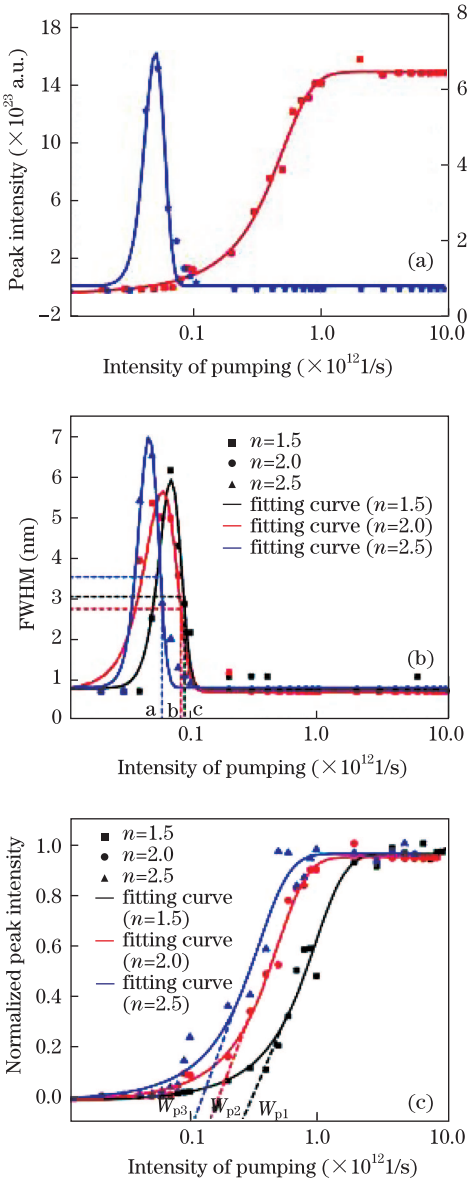

Fig. 2. (Color online) (a) Plots of peak intensity (red) and FWHM (blue) varying with a pumping rate of n_2=2.5; (b) FWHM varying with the pumping rate of different refractive indices, namely, 1.5 (black), 2 (red), and 2.5 (blue); (c) normalized peak intensity varying with the pumping rate of different refractive indices, namely, 1.5 (black), 2 (red), and 2.5 (blue).

without limiting the finite electronics in the atomic system. Hence, the peak intensity will be limited in a range, which is why the peak intensity will saturate.

We also calculated the emission spectra with the refractive indices of 1.5 and 2. According to the comparison of the results, the change trend is consistent with the trend of the spectra with a refractive index of 2.5. Therefore, we do not show the results here. To obtain the influence of the scattering media's refractive indices on random lasing, we show the peak intensity and the FWHM varying with the pumping rate at different refractive indices in Figs. 2(b) and (c), respectively. Here, we normalize the peak intensity for careful observation. Lasing threshold can be defined using many methods. Ito *et al.* first measured the curve of the spectral width of lasing emission varying with the pumping energy. Then, they found a pumping energy at which the spectral width became half of its maximum value. Such pumping energy was defined as the lasing threshold[24]. Using this method, we get the lasing threshold of the three curves in Fig. 2(b). As shown, the lasing thresholds of the three kinds of refractive indices are the pumping rates at the three points c, b, and a, which we define as W_c, W_b, and W_a, respectively. Apparently, we can get the expression $W_c > W_b > W_a$. In this letter, we also use the traditional method to determine the lasing threshold based on the curves of the peak intensity varying with pumping rate. Using the threshold values shown in Fig. 2(c), we can get the three lasing thresholds of the refractive indices of 1.5, 2, and 2.5, which are denoted as W_{p1}, W_{p2}, and W_{p3}, respectively. Obviously, they obey the expression $W_{p1} > W_{p2} > W_{p3}$. The two methods imply that the larger the refractive index of the scattering particles, the smaller the lasing threshold. When the refractive index of the scattering particles increases, the scattering intensity of particles becomes larger. The photons are more likely to be confined in the system and form closed-loop oscillation. Therefore, the loss of the open system and the lasing threshold are smaller.

In our experiment, we chose Rh6G as the gain medium and the Al particles as scattering medium. First, we evenly dispersed some Rh6G into a certain volume of glycol solution. Then, we added some Al particles into the solution. The concentrations of Al and Rh6G are 0.0015 and 0.02 mol/L, respectively. Here, we used glycol as a dispersant because the viscosity of the solution was relatively large. Therefore, the scattering particles can be evenly distributed in the solution.

Before the experiment, we first placed the sample into an ultrasonic oscillator for 30 min. Then, we poured the sample into a 1-mm-thick cuvette to form the quasi-2D disordered medium. The sample was then pumped using an optical parametric oscillator (OPO) whose center wavelength is 480 nm, pulse width is ~7 ns, and repetition rate is 10 Hz. The laser was focused into the solution using a lens whose focal length is 100 mm. The spectrum was obtained using a monochromator (SP2750, Princeton Instrument). The experimental scheme is shown in Fig. 3.

Figure 4(a) shows three typical spectra measured by a monochromator at pumping energies of 0.05, 0.61, 1.82, and 3.61 mJ, respectively. The diagram shows that the emission spectrum is wide when the pumping energy is small (0.05 and 0.61 mJ). When the energy is increased to 1.82 mJ, an obvious peak appears in the spectrum,

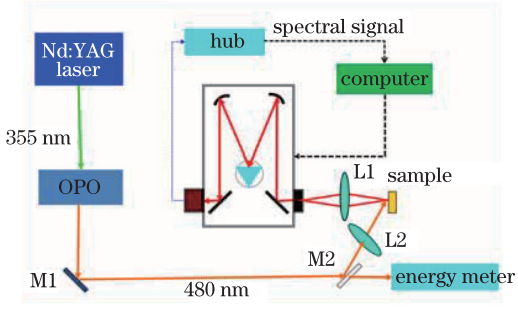

Fig. 3. Experimental setup.

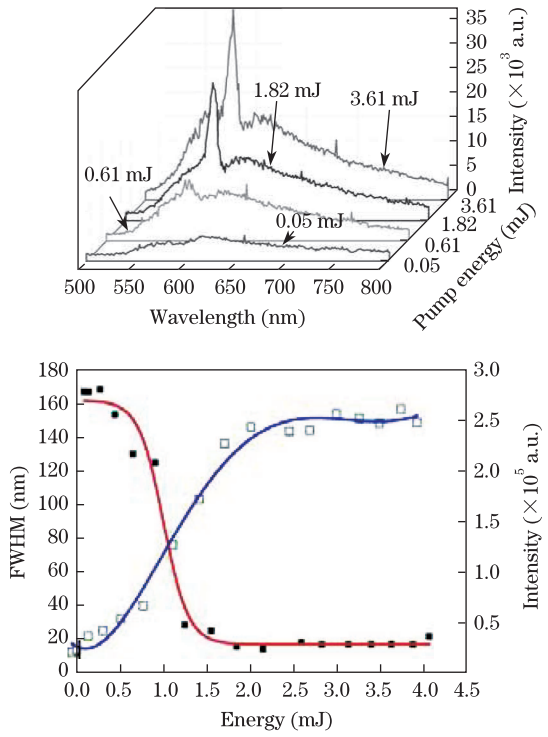

Fig. 4. (Color online) (a) Typical spectra of different pumping energies at 0.05, 0.61, 1.82, and 3.61 mJ; (b) peak intensity (blue) and FWHM (red) varying with pumping energy.

indicating a lasing action. Then, the peak intensity of the spectrum increases and the FWHM decreases. The dependence of peak intensity and FWHM on pumping energy is shown in Fig. 4(b). When energy is lower than 0.5 mJ, the peak intensity is small and FWHM is large. When the energy is larger than 0.5 mJ, the peak intensity exhibits an exponential growth and FWHM decreases dramatically. When the pumping energy reaches 1.5 mJ, the FWHM of the spectrum reaches a certain value and remains stable, but the peak intensity still increases. When the energy reaches 2.5 mJ, the peak intensity exhibits saturation. Comparing Figs. 4 and 2, we can conclude that the experimental results agree with the theoretical ones.

In conclusion, using the FDTD algorithm, we numerically solve Maxwell's equations and four-level rate equations and determine the dependence of the refractive indices of the scattering particles on random lasing in a 2D strongly disordered medium. The calculation results show that in low dimensional systems, the larger the difference of refractive indices between the scattering and background media, the stronger the feedback and the smaller the lasing threshold. We also confirm the existence of mode competition in a random laser. Based on the theoretical results, we perform an experiment. However, in contrast with the 2D system in the theoretical simulation, the sample system is leakier because it is more open. Hence, comparing the experimental and theoretical results quantitatively is difficult. Moreover, the experimental results agree with the calculated results qualitatively. These findings may be helpful in the realization of thin-film random lasers and planar waveguides with disorder.

The authors wish to thank Professor Jianguo Chen for the useful discussions and help. This work was supported by the Major Program of the National Natural Science Foundation of China (No. 60890200) and the National Science Association Foundation of China (No. 10976017).

References

1. S. John and G. Pang, Phys. Rev. A **54,** 3642 (1996).
2. D. Wiersma and A. Lagendijk, Phys. Rev. E **54,** 4256 (1996).
3. X. Jiang and C. M. Soukoulis, Phys. Rev. Lett. **85,** 70 (2000).
4. C. Vanneste and P. Sebbah, Phys. Rev. Lett. **87,** 183903 (2001).
5. X. Jiang and C. M. Soukoulis, Phy. Rev. E **65,** 25601 (2002).
6. J. Liu, Z. Xiong, and W. Chun, J. Opt. A Pure: Appl. Opt. **9,** 658 (2007).
7. J. Andreasen, A. A. Asatryan, L. C. Botten, M. A. Byrne, H. Cao, L. Ge, L. Labonte, P. Sebbah, A. D. Stone, H. E. Tureci, and C. Vanneste, Adv. Opt. Photon. **3,** 88 (2011).
8. O. Zaitsev and L. Deych, J. Optics **12,** 024001 (2010).
9. J. Andreasen, C. Vanneste, L. Ge, and H. Cao, Phys. Rev. A **81,** 043818 (2010).
10. N. M. Lawandy, R. Balachandran, A. Gomes, and E. Sauvain, Nature **368,** 436 (1994).
11. H. Cao, Y. Zhao, S. Ho, E. Seelig, Q. Wang, and R. Chang, Phys. Rev. Lett. **82,** 2278 (1999).
12. H. Cao, J. Xu, D. Zhang, S. Chang, S. Ho, E. Seelig, X. Liu, and R. Chang, Phys. Rev. Lett. **84,** 5584 (2000).
13. H. Cao, J. Xu, S. Chang, and S. Ho, Phys. Rev. E **61,** 1985 (2000).
14. Y. Ling, H. Cao, A. Burin, M. Ratner, X. Liu, and R. Chang, Phys. Rev. A **64,** 63808 (2001).
15. K. Van Der Molen, R. Tjerkstra, A. Mosk, and A. Lagendijk, Phy. Rev. Lett. **98,** 143901 (2007).
16. Q. Song, S. Xiao, Z. Xu, J. Liu, X. Sun, V. Drachev, V. M. Shalaev, O. Akkus, and Y. L. Kim, Opt. Lett. **35,** 1425 (2010).
17. J. Kitur, G. Zhu, M. Bahoura, and M. A. Noginov, J. Optics **12,** 024009 (2010).
18. T. Zhai, X. Zhang, Z. Pang, X. Su, H. Liu, S. Feng, and L. Wang, Nano Lett. **11,** 4295 (2011).
19. P. Sebbah and C. Vanneste, Phys. Rev. B **66,** 144202 (2002).
20. Y. Xie, B. Li, Q. You, D. Hu, Y. Lei, H. Yang, and Y. Wang, in *Proceedings of Remote Sensing, Environment and Transportation Engineering (RSETE) 2011* 5904 (2011).
21. X. Zhai, Y. Sun, and D. Wu, Opt. Lett. **36,** 4242 (2011).
22. L. Yang, G. Feng, J. Yi, K. Yao, G. Deng, and S. Zhou, Appl. Opt. **50,** 1816 (2011).
23. J. Berenger, J. Comput. Phys. **114,** 185 (1994).
24. T. Ito and M. Tomita, Phys. Rev. E **66,** 027601 (2002).